Hybrid Trypsinized Nucleosomal Arrays: Identification of Multiple Functional Roles of the H2A/H2B and H3/H4 N-Termini in Chromatin Fiber Compaction[†]

Christin Tse and Jeffrey C. Hansen*

Department of Biochemistry, The University of Texas Health Science Center at San Antonio, 7703 Floyd Curl Drive, San Antonio, Texas 78284-7760

Received April 7, 1997; Revised Manuscript Received July 18, 1997[⊗]

ABSTRACT: A defined 12-mer nucleosomal array in solution exists in a complex equilibrium between an unfolded 29S conformation, a 40S folding intermediate, an extensively folded 55S conformation, and soluble oligomeric states formed from cooperative intermolecular association of individual 12-mer arrays. Proteolytic removal of all of the core histone N-terminal tail domains previously has been shown to abolish both salt-dependent nucleosomal array folding and oligomerization. To elucidate the individual contributions of the H2A/H2B and H3/H4 tail domains to nucleosomal array condensation, "hybrid" trypsinized nucleosomal arrays have been assembled from tandemly repeated 5S rDNA and either trypsinized H3/H4 tetramers and intact H2A/H2B dimers or trypsinized H2A/H2B dimers and intact H3/H4 tetramers. Neither of the hybrid trypsinized arrays formed either the 40S or the 55S folded conformations in 2 mM $MgCl_2$. In ≥4 mM $MgCl_2$, however, both fully trypsinized arrays and each hybrid trypsinized array formed the 40S folding intermediate, but not the 55S conformation. In contrast to folding, each hybrid trypsinized nucleosomal array oligomerized completely in $MgCl_2$. These studies have identified three mechanistically distinct functions performed by the core histone N-termini during salt-dependent condensation of nucleosomal arrays. The complexity of tail domain function in chromatin is discussed in the context of a competitive interaction model in which the core histone N-termini provide direct mechanistic links between the structure and function of the chromatin fiber.

Several distinct layers of packaging are required to achieve the level of DNA compaction found in eukaryotic chromosomes. At the initial level, chromosomal DNA is assembled with core histone octamers to form a long contiguous nucleosomal array that is 10 nm in diameter and consists of 10^5-10^9 nucleosomal subunits. Throughout much of the genome, local folding of the nucleosomal array is believed to produce a condensed 30 nm diameter chromatin fiber (van Holde, 1988; Wolffe, 1995). This level of compaction accounts for an ∼50-fold reduction in fiber length and is a targeted site for regulation of transcription, replication, and repair [reviewed in Wolffe (1995) and Fletcher and Hansen (1996)]. Longer-range looping and twisting of the nucleosomal array subsequently leads to the formation of the highly condensed 200−400 nm diameter domains characteristic of interphase chromosomal fibers (Boy de la Tour & Laemmli, 1988; Belmont et al., 1989; Belmont & Bruce, 1994). Very little is known about the macromolecular determinants of interphase chromosome structure. Whereas topoisomerase II and the XCAP family of proteins are required for the terminal condensation of metaphase chromosomes (Hirano, 1994), no equivalent proteins have been identified for condensation of interphase chromosomal fibers. In addition, it has recently been shown that depletion of linker histones from either isolated metaphase chromosomes (Ohsumi et al., 1993), isolated intact nuclei (Dasso et al., 1994), or living cells (Bouvet et al., 1994; Shen et al., 1995) does not dramatically alter interphase chromosome size or morphology. The simplest explanation for these results is that much of the ability to condense into interphase chromosomal fibers lies within the nucleosomal array itself.

To determine the contributions of the nucleosomal array to chromosomal fiber condensation, we have been systematically characterizing the solution-state conformational dynamics of a defined 12-mer nucleosomal array model system consisting of only core histone octamers and tandemly repeated 5S DNA (Simpson et al., 1985). The behavior of these nucleosomal arrays in solution is quite complex. In "physiological" cationic conditions (e.g., 100 mM Na^+, 2 mM Mg^{2+}), each 12-mer nucleosomal array monomer is in equilibrium between unfolded, moderately folded, and extensively folded conformations (Schwarz & Hansen, 1994; Schwarz et al., 1996). In addition, the 12-mer arrays also are in equilibrium with soluble oligomeric states formed by reversible cooperative self-association of array monomers (Schwarz et al., 1996). In the absence of salt, the equilibrium favors the unfolded conformational state of the array monomer. However, as the salt concentration is increased, the equilibrium is shifted first toward intramolecular folding, and then toward oligomerization (Schwarz & Hansen, 1994; Schwarz et al., 1996). Oligomerization occurs independently of whether the arrays are folded or unfolded (Schwarz et al., 1996), indicating that folding and oligomerization are not strictly coupled. Extrapolation of the solution-state behavior of the 12-mer nucleosomal array to that of a chromosome length array strongly suggests that many of the fundamental properties necessary to achieve bulk chromosome level condensation are intrinsic within the core histones of the chromosomal nucleosomal array [Schwarz et al., 1996; reviewed in Fletcher and Hansen (1996)].

[†] Supported by NIH Grant GM45916.

* To whom correspondence should be addressed. Telephone: (210) 567-6980. FAX: (210) 567-6595. E-mail: hansen@bioc02.uthscsa.edu.

[⊗] Abstract published in *Advance ACS Abstracts,* September 1, 1997.

S0006-2960(97)00801-5 CCC: $14.00

Recent studies indicate that the core histone N-terminal "tail" domains provide essential functions required for nucleosomal array condensation. Nucleosomal arrays reconstituted from trypsinized histone octamers lacking all of their N-terminal tail domains can neither fold (Garcia-Ramirez et al., 1992; Fletcher & Hansen, 1995) nor oligomerize (Schwarz et al., 1996) in physiological cationic conditions. However, the mechanisms through which the tail domains modulate folding and oligomerization clearly are not simple. In a nucleosomal array that is unfolded in low salt, the tail domains interact with nucleosomal core DNA to facilitate the wrapping of DNA around each histone octamer (Garcia-Ramirez et al., 1992; Fletcher & Hansen, 1995). However, recent experiments have revealed that the tail domains do not remain bound to core DNA during salt-dependent folding and oligomerization; i.e., they undergo specific function-linked rearrangement (Usachenko et al., 1994; Fletcher & Hansen, 1995). Additional studies have shown that while H3/H4 tetramer arrays are incapable of salt-dependent folding (Hansen & Wolffe, 1994), they readily oligomerize in the same $MgCl_2$ range as intact arrays (Schwarz et al., 1996). Cumulatively, these results have led us to hypothesize that folding and oligomerization are mediated by different sets of histone tail domains, and that more than a single mechanism of action is involved in tail domain function in chromatin (Fletcher & Hansen, 1995; Schwarz et al., 1996; Hansen, 1997).

To address these hypotheses, in the present work "hybrid" trypsinized nucleosomal arrays have been constructed that specifically lacked only the H2A/H2B or H3/H4 tail domains. The ability of the hybrid nucleosomal arrays to fold and oligomerize was compared against the behavior of intact or fully trypsinized nucleosomal arrays. Results directly demonstrate that the H3/H4 and H2A/H2B N-termini mediate the solution-state conformational dynamics of nucleosomal arrays through at least three distinct molecular mechanisms. The biological relevance of these results is discussed in terms of a competitive interaction model in which the tail domains provide direct macromolecular links between the structural and functional properties of the chromosomal fiber.

EXPERIMENTAL PROCEDURES

Materials. The 208-12 DNA template consists of 12 tandem repeats of a 208 bp sequence derived from the *Lytechinus* 5S rRNA gene (Simpson et al., 1985). This template was grown and purified from the pPOL208-12 plasmid as described previously (Schwarz & Hansen, 1994). Whole chicken blood was purchased from Pel-Freeze Biologicals and used as the source of histone octamers. Trypsin immobilized on DITC-treated glass beads and soybean trypsin inhibitor were obtained from Sigma. All other chemicals were of reagent grade.

Purification of Native and Trypsinized Histone Octamers, H3/H4 Tetramers, and H2A/H2B Dimers. Native oligonucleosomes were isolated from chicken erythrocyte nuclei as described (Hansen et al., 1989). Trypsinized oligonucleosomes were obtained by treating native oligonucleosomes with immobilized trypsin essentially as described by Ausio et al. (1989). Briefly, immobilized trypsin beads were resuspended in 10 mM Tris-HCl, 50 mM NaCl, and 0.25 mM EDTA, pH 7.8, overnight at 4 °C. The immobilized trypsin was then incubated with native oligonucleosomes at a ratio of 10 mg of trypsin per 1 mg of oligonucleosomes and mixed by gentle rotation at room temperature for varying lengths of times. The reaction was quenched by filtering the oligonucleosomes through a 0.2 μm filter and subsequent addition of soybean trypsin inhibitor (Sigma). Test digests were performed to determine the digestion lengths necessary to exclusively generate the P1−P5 peptides described by Bohm and Crane-Robinson (1984) (Table 1). Large-scale oligonucleosome digests subsequently were performed under identical conditions. Native and trypsinized histone octamers, H3/H4 tetramers, and H2A/H2B dimers were purified from their respective oligonucleosomes using the hydroxyapatite method of Simon and Felsenfeld (Simon, 1979). Pure fractions were pooled and stored at 4 °C at a concentration of ~0.40 mg/mL, as determined from the A_{230} (Stein, 1979).

Oligonucleosome Reconstitution. Throughout this paper, nucleosomal arrays reconstituted with native histone octamers are referred to as "intact" nucleosomal arrays while those reconstituted with the P1−P5 peptides are referred to as "fully trypsinized" nucleosomal arrays. Intact and fully trypsinized 208-12 nucleosomal arrays were reconstituted by combining the 208-12 DNA template and either intact or trypsinized core histone octamers according to the salt dialysis method described by Hansen and Lohr (1993). The molar ratio of histone octamers to 208 bp DNA ranged from 1.1 to 1.3. The final DNA concentration was 100 μg/mL. The final dialysis step was into 10 mM Tris-HCl, 0.25 mM EDTA, and 2.5 mM NaCl, pH 7.8 (TE), buffer.

Nucleosomal arrays in which only the H2A/H2B dimers or H3/H4 tetramer components of the nucleosomal subunits were trypsinized are referred to as "hybrid trypsinized" nucleosomal arrays. Assembly of the two different hybrid trypsinized nucleosomal arrays was achieved as follows. In the case of the hybrid nucleosomal arrays lacking H2A/H2B tail domains, intact H3/H4 tetramers and trypsinized H2A/H2B dimers were added to the 208-12 DNA at a molar ratios of histone to 208 bp repeat of (1.1−1.3):1 and (2.2−2.6):1, respectively. All other aspects of the salt dialysis reconstitution were the same as described above. The hybrid nucleosomal arrays lacking H3/H4 tail domains were constructed from trypsinized H3/H4 tetramers and intact H2A/H2B dimers using the same strategy. The extent of template saturation achieved after reconstitution was determined by sedimentation velocity analysis and *Eco*RI digestion (Table 2).

Analytical Ultracentrifugation. Sedimentation velocity experiments were performed using a Beckman XL-A analytical ultracentrifuge equipped with scanner optics as described (Schwarz & Hansen, 1994). The A_{260} of the samples was between 0.6 and 0.8. The integral distribution of sedimentation coefficients was determined by the method of van Holde and Weischet (1978) using Ultrascan data analysis software version 2.94.

Differential Centrifugation Assay for Nucleosomal Array Oligomerization. The ability of the various nucleosomal arrays to oligomerize in the presence of $MgCl_2$ was determined by differential centrifugation as described previously (Schwarz et al., 1996).

EcoRI Digestion Assay. Two micrograms of nucleosomal arrays was digested with 15 units of *Eco*RI for 60 min at room temperature in digestion buffer H (Promega), and reactions were quenched with an equal volume of 2× loading buffer (10% glycerol, 10 mM EDTA, and 0.3% bromophenol

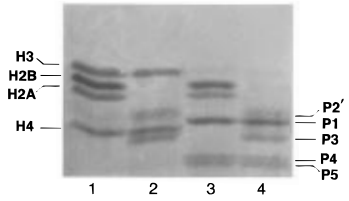

FIGURE 1: Histone content of reconstituted nucleosomal arrays. Intact and trypsinized reconstitutes were electrophoresed on an 18% SDS−polyacrylamide gel and bands visualized using a Bio-Rad silver staining kit. Intact and fully trypsinized nucleosomal arrays were loaded in lanes 1 and 4, respectively. Hybrid trypsinized arrays reconstituted with intact histones H3/H4 and trypsinized histones H2A/H2B were loaded in lane 2. Hybrid trypsinized arrays reconstituted with intact histones H2A/H2B and trypsinized histones H3/H4 were loaded in lane 3. Bands designated H3, H2B, H2A, and H4 represent the intact core histones. Bands designated as P1−5 refer to the trypsinized peptides defined previously by Bohm and Crane-Robinson (1984) (Table 1).

Table 1: Amino Acid Composition of Intact and Trypsinized Core Histones

	H2A	H2B	H3	H4
intact	1−128[a]	1−126	1−135	102
trypsinized	12−118 (P2')[b]	24−125 (P3)	27−129 (P1)	18/20−102 (P4/P5)

[a] Numbers indicate the amino acid residues present before and after proteolytic digestion with trypsin. The first and last numbers represent the N- and C-termini, respectively. [b] The P1−P5 designations refer to the trypsinized fragments characterized previously by Bohm and Crane Robinson (1984).

blue). Samples were then electrophoresed on a 0.8% agarose gel buffered with 45 mM Tris−borate, 1 mM EDTA for 3 h at 1 V/cm to resolve histone-free DNA repeats from nucleosome monomers and larger undigested oligonucleosome fragments (Hansen et al., 1989; Meersseman et al., 1991). The percent of histone-free DNA repeats present in each sample was calculated by quantitating the ethidium signal from each gel band using densitometry and multiplying the signal from the nucleosomal bands by 2.5 to correct for histone quenching of ethidium fluorescence (McMurray & van Holde, 1985).

RESULTS

Assembly of Saturated Preparations of Intact, Fully Trypsinized, and Hybrid Trypsinized 208-12 Nucleosomal Arrays. To determine the histone composition of the intact, fully trypsinized, and hybrid trypsinized nucleosomal arrays after reconstitution, samples were electrophoresed on a denaturing SDS−polyacrylamide gel and histone bands visualized by silver staining (Figure 1). The bands labeled P1−P5 in the fully trypsinized nucleosomal array sample (lane 4) correspond to the histone polypeptide fragments characterized previously (Bohm & Crane-Robinson, 1984; see Table 1). The sample electrophoresed in lane 2 consisted of intact histones H3/H4 and trypsinized histones H2A/H2B (P2′ and P3), while that in lane 3 consisted of trypsinized histones H3/H4 (P1 and P4/P5) and intact histones H2A/H2B. Thus, the data in Figure 1 confirm that the desired histone content of the fully trypsinized and hybrid trypsinized nucleosomal arrays had been achieved after reconstitution. Verification that the hybrid trypsinized nucleosomal arrays were assembled into nucleosomal structures was accomplished by micrococcal nuclease digestion. Extensive digestion of intact, fully trypsinized, and both of the hybrid trypsinized nucleosomal arrays each yielded distinct mono- and dinucleosomal bands (data not shown).

Table 2: Properties of Intact, Fully Trypsinized, and Hybrid Trypsinized 208-12 Nucleosomal Arrays

property	intact	+H3/H4[a]	+H2A/H2B[b]	fully trypsinized
% free DNA[c]	2.1 ± 0.3	4.3 ± 0.6	3.5 ± 0.3	4.9 ± 1.0
$s_{20,w}$[d] (S)	29	27	28.5	25
55S structure formation[e]	yes	no	no	no
oligomerization[f]	+++	++	+	−

[a] Refers to the hybrid trypsinized nucleosomal array preparation reconstituted from native H3/H4 tetramers and trypsinized H2A/H2B dimers. [b] Refers to the hybrid trypsinized nucleosomal array preparation reconstituted from native H2A/H2B dimers and trypsinized H3/H4 tetramers. [c] Values indicate the mean ± the standard deviation of the percentage of unoccupied 5S rDNA repeats in two different reconstitutes having the indicated sedimentation coefficients as determined by the *Eco*RI digestion assay (see Experimental Procedures). [d] Values indicate the average $s_{20,w}$ determined at the boundary midpoint of each reconstitute in low-salt TE buffer. [e] Refers to the ability to form the 55S structure in $MgCl_2$ prior to oligomerization. [f] Refers to the efficiency of Mg^{2+}-dependent oligomerization. The latter two properties are summarized from the data shown in Figures 2−5.

Subsaturated 208-12 nucleosomal arrays fold to a lesser extent (Hansen & Lohr, 1993; Schwarz & Hansen, 1994; Fletcher et al., 1994b) and oligomerize at higher [$MgCl_2$] (Schwarz et al., 1996) than intact arrays saturated with 12 histone octamers. Thus, it was very important to determine the degree of template saturation of each reconstitute. This was accomplished using a combination of sedimentation velocity analysis in TE buffer and *Eco*RI digestion. The utility of each of these assays for determining saturation has been established previously (Hansen et al., 1989; Meersseman et al., 1991; Pennings et al., 1991; Hansen & Lohr, 1993). In the case of *Eco*RI, the DNA digestion sites flank the majority of nucleosomes positioned on the 208-12 DNA (Hansen et al., 1989; Dong et al., 1990; Meersseman et al., 1991). Thus, digestion of intact 208-12 nucleosomal arrays with *Eco*RI yields a mixture of unoccupied 5S repeats, mononucleosomes, and a fraction of partially digested oligomers (e.g., dimers, trimers), the latter resulting from nucleosome positioning heterogeneity (Hansen et al., 1989; Dong et al., 1990; Meersseman et al., 1991; Pennings et al., 1991). When the fully trypsinized and hybrid trypsinized nucleosomal arrays were digested with *Eco*RI, each of the aforementioned species was observed after electrophoresis on agarose (data not shown). Consistent with the results of Ausio et al. (1989), each of the hybrid mononucleosomes exhibited an intermediate migration relative to the intact and fully trypsinized mononucleosomes.

Quantitation of the amount of histone-free 5S repeats liberated by *Eco*RI digestion and the results of the sedimentation velocity analysis are summarized in Table 2. The sedimentation coefficient in TE buffer of an unfolded 208-12 nucleosomal array saturated with 12 intact histone octamers is 29 S (Hansen et al., 1989; Schwarz & Hansen, 1994), while an array saturated with 12 fully trypsinized histone octamers is 25 S (Fletcher & Hansen, 1995). Based on sedimentation coefficient distribution analyses, "saturated" reconstituted preparations typically consist of 50−75% of the DNA templates loaded with 12 octamers while the remaining templates contain 11 octamers (Hansen et al.,

1989; Hansen & Lohr, 1993; Schwarz & Hansen, 1994). It should be noted that while such a preparation would have an average sedimentation coefficient measured at the boundary midpoint of 29 S or 25 S for intact or trypsinized arrays, respectively, ~2−5% of the total *Eco*RI digestion products would resolve on gels as histone-free 5S repeats due to the small fraction of slightly subsaturated templates present in the sample. Precisely such results were obtained for both the intact and fully trypsinized 208-12 nucleosomal arrays used in these studies (Table 2). Importantly, the amount of histone-free 5S DNA repeats liberated from each of the hybrid trypsinized nucleosomal array preparations was virtually identical to the amounts released from the intact and fully trypsinized nucleosomal arrays (Table 2). These results indicate that the folding and oligomerization studies described below were performed with equivalently saturated preparations of intact, fully trypsinized, and hybrid trypsinized nucleosomal arrays in which ~50−75% of the DNA templates contained 12 histone octamers.

The data in Table 2 also provide additional insight into the functions contributed by the tail domains within nucleosomal arrays that are unfolded in low salt. Previous studies have shown that the tail domains of unfolded nucleosomal arrays bind to nucleosomal core DNA and help mediate complete wrapping of the core DNA around each histone octamer (Garcia-Ramirez et al., 1992; Fletcher & Hansen, 1995). Experimentally, this is reflected by the fact that saturated intact 208-12 nucleosomal arrays sediment at 29 S in low salt while fully trypsinized saturated arrays sediment at 25 S under these conditions (Table 2; Fletcher & Hansen, 1995). The sedimentation coefficient in low salt of saturated hybrid nucleosomal arrays containing only the H3/H4 tail domains was 27 S while that of saturated hybrid nucleosomal arrays containing only the H2A/H2B tail domains was 28.5 S (Table 2). These results demonstrate directly that in low salt the H2A/H2B tail domains stabilize wrapping of the core DNA near the entry and exit points of each nucleosomal subunit. By inference, they also indicate that the H3/H4 tail domains help stabilize wrapping of the more central nucleosomal core DNA in low salt. These conclusions are consistent both with previous analyses of hybrid trypsinized core particles (Ausio et al., 1989) and with modeling studies of the crystallized histone octamer (Moudrianakis & Arents, 1993).

Mg^{2+}-Dependent Nucleosomal Array Oligomerization. Under the more physiological salt conditions that promote folding and oligomerization, nucleosomal core DNA wrapping is mediated by inorganic cations, and the tail domains rearrange to noncore DNA location(s) (Usachenko et al., 1994; Fletcher & Hansen, 1995). Consequently, our primary goal was to characterize the folding and oligomerization of hybrid trypsinized nucleosomal arrays in the presence of $MgCl_2$. Folding and oligomerization occur hierarchically with increasing [Mg^{2+}] (Schwarz et al., 1996; Schwarz & Hansen, 1994). Thus, it was first necessary to establish the extent of oligomerization as a function of $MgCl_2$ concentration using the differential centrifugation assay. The ability of the various nucleosomal arrays to oligomerize in $MgCl_2$ is shown in Figure 2. Oligomerization was indicated by a decrease in the A_{260} of the supernatant after centrifugation in the microcentrifuge (Schwarz et al., 1996; Schwarz & Hansen, 1994). The global mechanism that underlies this behavior involves reversible, cooperative formation of large

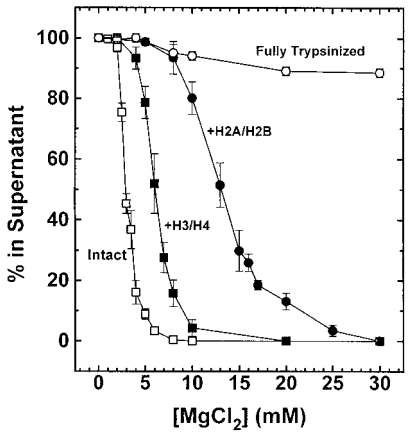

FIGURE 2: Mg^{2+}-dependent oligomerization of intact and trypsinized nucleosomal arrays. Shown is the percent of the original sample that remained in the supernatant after centrifugation for 10 min at 16000*g* in a microcentrifuge. Each data point represents the mean ± the standard deviation of 5−10 determinations. Intact nucleosomal arrays (□); fully trypsinized nucleosomal arrays (○); hybrid nucleosomal arrays containing intact histones H3/H4 and trypsinized histones H2A/H2B (■, +H3/H4); hybrid nucleosomal arrays containing intact histones H2A/H2B and trypsinized histones H3/H4 (●, +H2A/H2B).

soluble nucleosomal array oligomers that increase in size as the $MgCl_2$ concentration is increased (Schwarz et al., 1996). At the concentrations used in these studies, intact nucleosomal arrays did not oligomerize between 0 and 2 mM. However, they were 50% oligomerized in ~3 mM and completely oligomerized in ~6 mM $MgCl_2$. Trypsinized nucleosomal arrays were essentially incapable of forming oligomers at any $MgCl_2$ concentration, consistent with previous results (Schwarz et al., 1996). Interestingly, both hybrid nucleosomal arrays were capable of Mg^{2+}-dependent oligomerization, albeit at higher $MgCl_2$ concentrations than observed for intact nucleosomal arrays (Figure 2). Oligomerization of hybrid nucleosomal arrays containing only their H3/H4 tail domains was half-maximal at ~6 mM $MgCl_2$, while those containing only the H2A/H2B domains achieved half-maximal oligomerization at ~13 mM $MgCl_2$. In addition, both the onset and completion of oligomerization of the hybrid arrays were shifted to higher $MgCl_2$ concentrations. Despite these differences, oligomerization of both hybrid trypsinized nucleosomal arrays appeared to remain cooperative as judged from the steep oligomerization profiles (Figure 2). These results indicate that only one set of tail domains is absolutely required to mediate Mg^{2+}-dependent nucleosomal array oligomerization, and that both the H3/H4 and H2A/H2B tail domains can fulfill this purpose. The data in Figure 2 further demonstrate that the H3/H4 tail domains are significantly more efficient at mediating oligomerization than the H2A/H2B tail domains.

Mg^{2+}-Dependent Nucleosomal Array Folding. The ability of the various nucleosomal arrays to undergo Mg^{2+}-dependent folding was determined by sedimentation velocity analysis in the analytical ultracentrifuge. Numerous previous studies have established that intact 208-12 nucleosomal arrays in divalent cation solutions are in equilibrium between the 29S unfolded state, a 40S folding intermediate whose extent of compaction is equivalent to a moderately folded contacting zig-zag or open helical structure, and an extensively folded 55S conformation whose extent of compaction is equivalent to a maximally condensed contacting helix

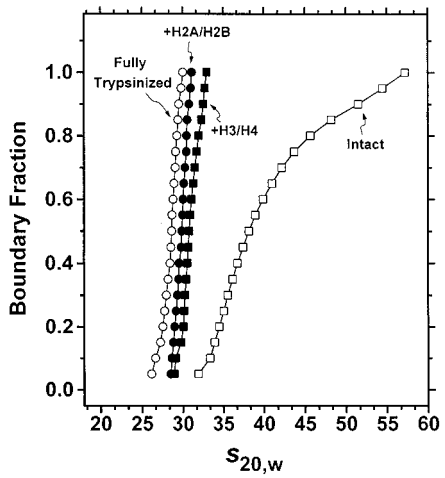

FIGURE 3: Sedimentation velocity analysis of intact and trypsinized nucleosomal arrays in 2.0 mM $MgCl_2$. Samples in TE buffer containing 2.0 mM $MgCl_2$ were equilibrated at 21 °C and sedimented at 20 000 rpm. Shown are the sedimentation coefficient distributions obtained after analysis of the boundaries by the method of van Holde and Weischet (1978). Intact nucleosomal arrays (□); fully trypsinized nucleosomal arrays (○); hybrid nucleosomal arrays containing intact histones H3/H4 and trypsinized histones H2A/H2B (■, +H3/H4); hybrid nucleosomal arrays containing intact histones H2A/H2B and trypsinized histones H3/H4 (●, +H2A/H2B).

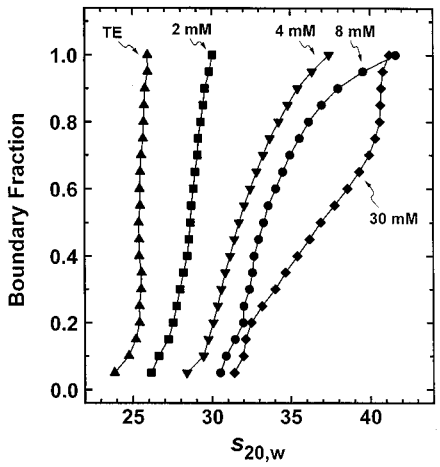

FIGURE 4: Sedimentation velocity analysis of fully trypsinized nucleosomal arrays at elevated $MgCl_2$ concentrations. Fully trypsinized nucleosomal arrays were equilibrated at 21 °C and sedimented at 20 000 rpm. Shown are the sedimentation coefficient distributions obtained in TE buffer containing 0 mM (▲), 2.0 mM (■), 4.0 mM (▼), 8.0 mM (●), or 30 mM (◆) $MgCl_2$.

(Hansen et al., 1989; Garcia-Ramirez et al., 1992; Hansen & Wolffe, 1992; Schwarz & Hansen, 1994; Fletcher et al., 1994b; Fletcher & Hansen, 1995; Schwarz et al., 1996). Importantly, although 208-12 nucleosomal arrays can form the 40S and 55S conformations in the presence of divalent cations, the folded structures are unstable in the absence of other macromolecular factors (e.g., histone H1). This leads to the broad sedimentation coefficient distributions indicative of equilibration between unfolded and extensively folded states (Schwarz & Hansen, 1994; see Figure 3). It should be noted that while the exact nature of highly condensed folded chromatin structures remains unresolved [reviewed in Woodcock (1995), van Holde and Zlatanova (1995), and Fletcher and Hansen (1996)], the analytical ultracentrifuge provides an unequivocal assay for the *extent* of folding of the 208-12 system in solution (Hansen et al., 1994, 1997), and it is in this context in which all of the folding studies described below are interpreted. For each nucleosomal array type, folding was examined in the salt range that preceded the onset of oligomerization, i.e., ≤2 mM $MgCl_2$ for intact arrays, ≤4 mM $MgCl_2$ for hybrid arrays containing H3/H4 tail domains, and ≤8 mM $MgCl_2$ for hybrid arrays containing H2A/H2B tail domains. Fully trypsinized nucleosomal arrays do not oligomerize and were studied in the range of 2−30 mM $MgCl_2$.

As a control, intact and fully trypsinized 208-12 nucleosomal arrays were first sedimented in 2 mM $MgCl_2$. Consistent with previous results (Schwarz & Hansen, 1994; Schwarz et al., 1996), the intact arrays yielded the characteristic broad biphasic sedimentation coefficient distribution indicative of equilibration between the 29S, 40S, and 55S conformational states (Figure 3). In contrast, the sedimentation coefficient distribution of fully trypsinized nucleosomal arrays ranged from 26 to 30 S (Figure 3), indicating that they remained unfolded in 2 mM $MgCl_2$ (Fletcher & Hansen, 1995). Each of the hybrid trypsinized nucleosomal arrays subsequently was sedimented in 2 mM $MgCl_2$ to determine whether arrays containing only the H3/H4 or H2A/H2B tail domains could mimic the folding behavior of the intact arrays. Under these ionic conditions, the sedimentation coefficient distribution of hybrid nucleosomal arrays containing only H3/H4 tail domains ranged from 29 to 33 S, while that of the hybrids containing only H2A/H2B tail domains ranged from 29 to 31 S (Figure 3). Thus, neither of the hybrid trypsinized arrays was able to fold in 2 mM $MgCl_2$.

Further insight into tail domain function in chromatin folding was revealed by studies of trypsinized nucleosomal arrays in ≥2 mM $MgCl_2$ concentrations. Recall that these experiments could be performed because the hybrid trypsinized arrays oligomerized at higher $MgCl_2$ concentrations than intact arrays, while the fully trypsinized arrays did not oligomerize at all (Figure 2). The sedimentation coefficient distributions of fully trypsinized nucleosomal arrays in 4−30 mM $MgCl_2$ are shown in Figure 4. Although fully trypsinized arrays were unfolded in 2 mM $MgCl_2$, they yielded sedimentation coefficient profiles characteristic of equilibration between the 29S unfolded conformation and the 40S folding intermediate in 4−30 mM $MgCl_2$. That is, the average sedimentation coefficient measured at the boundary midpoint (boundary fraction = 0.5) increased continuously with increasing $MgCl_2$, while the sedimentation coefficients in the upper region of the distribution profiles (i.e., boundary fraction = 0.6−1.0) reached a maximum of ∼40 S in 30 mM $MgCl_2$. The latter observation indicates that an ∼40S structure is the limiting conformation formed under these high-salt conditions. It should be noted that maximum compaction was observed in 30 mM $MgCl_2$; at higher concentrations, the sedimentation coefficients of trypsinized nucleosomal arrays *decreased* with increasing $MgCl_2$ (data not shown). Importantly, these results demonstrate that the tail domains are not absolutely essential for formation of the 40S conformation in high $MgCl_2$ concentrations. Furthermore, despite being able to form the 40S folding intermediate, under no conditions were fully trypsinized nucleosomal arrays capable of forming the highly condensed 55S conformation.

At the highest $MgCl_2$ concentrations that could be studied prior to oligomerization, both types of hybrid trypsinized

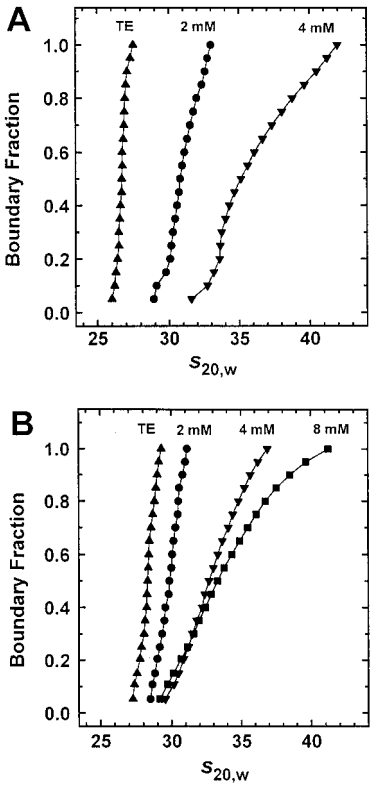

FIGURE 5: Sedimentation velocity analysis of hybrid trypsinized nucleosomal arrays at elevated $MgCl_2$ concentrations. Samples were equilibrated at 21 °C and sedimented at 20 000 rpm. (A) Hybrid nucleosomal arrays containing intact histones H3/H4 and trypsinized histones H2A/H2B. Shown are the sedimentation coefficient distributions obtained in TE buffer containing 0 mM (▲), 2.0 mM (●), or 4.0 mM (▼) $MgCl_2$. (B) Hybrid nucleosomal arrays containing intact histones H2A/H2B and trypsinized histones H3/H4. Shown are the sedimentation coefficient distributions obtained in TE buffer containing 0 mM (▲), 2.0 mM (●), 4.0 mM (▼), or 8.0 mM (■) $MgCl_2$.

nucleosomal arrays yielded essentially the same results as the fully trypsinized nucleosomal arrays. Hybrid arrays containing only H3/H4 tail domains sedimented between 31 and 42 S in 4 mM $MgCl_2$ (Figure 5A), while the hybrid arrays containing only H2A/H2B tail domains sedimented between 29 and 37 S in 4 mM $MgCl_2$ and between 29 and 41 S in 8 mM $MgCl_2$ (Figure 5B). Thus, in contrast to intact nucleosomal arrays, neither of the hybrid arrays were capable of forming the maximally folded 55S conformation prior to the onset of oligomerization. As judged by the sedimentation coefficient distribution profiles in 4 and 8 mM $MgCl_2$, there was no significant difference between the extent of compaction of the fully trypsinized arrays and the hybrid arrays containing only the H2A/H2B tail domains. In contrast, in 4 mM $MgCl_2$ the equilibrium was shifted significantly further toward the 40S state for the hybrid arrays containing only the H3/H4 tail domains (Figure 6).

DISCUSSION

Despite extensive investigation, both the functional roles and molecular mechanisms of action of the core histone N-terminal tail domains in chromatin have long remained enigmatic [reviewed in Wolffe (1995) and Fletcher and Hansen (1996)]. Most previous studies of tail domain function have been performed with nucleosome cores, and subsequently have focused on the consequences of tail domain interaction with core DNA. However, it has recently

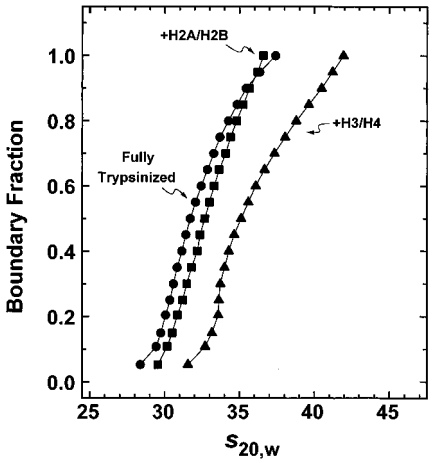

FIGURE 6: Direct comparison of the extent of folding of fully trypsinized and hybrid trypsinized nucleosomal arrays in 4 mM $MgCl_2$. Shown are the sedimentation coefficient distributions in 4 mM $MgCl_2$ of fully trypsinized nucleosomal arrays (●), hybrid arrays containing intact histones H2A/H2B and trypsinized histones H3/H4 (■, +H2A/H2B), and hybrid arrays containing intact histones H3/H4 and trypsinized H2A/H2B (▲, +H3/H4). Distribution profiles were replotted from the data in Figures 4 and 5, respectively.

been demonstrated that both the functions and the locations of the tail domains in nucleosome core particles and unfolded nucleosomal arrays in low salt differ significantly from those in nucleosomal arrays that are condensed in physiological salt [Garcia-Ramirez et al., 1992; Fletcher & Hansen, 1995; Schwarz et al., 1996 reviewed in Fletcher and Hansen (1996) and Hansen (1997)]. Thus, it has become increasingly important to study tail domain function under conditions that are more relevant to those found in vivo. The present studies have addressed this need by determining the individual functions of the H2A/H2B and H3/H4 N-terminal domains in salt-dependent nucleosomal array folding and oligomerization.

Complexity of N-Terminal Tail Domain Function during Nucleosomal Array Condensation. Neither the fully trypsinized nor the hybrid trypsinized nucleosomal arrays are capable of folding in 2 mM $MgCl_2$ (Figure 3). By contrast, intact nucleosomal arrays are capable of forming both the 40S and 55S folded structures under the same ionic conditions (Figure 3). Importantly, this indicates that the H2A/H2B and H3/H4 tail domains both are essential for intact nucleosomal arrays to fold into the maximally condensed 55S conformation. In >2 mM $MgCl_2$, both the fully trypsinized and the two hybrid nucleosomal arrays exhibited continuous salt-dependent increases in the extent of folding, ultimately leading to the formation of a limiting ~40S folded structure (Figures 4 and 5). The 40S conformation is formed from close approach of adjacent nucleosomal subunits (Hansen & Lohr, 1993; Fletcher et al., 1994b). The fact that fully trypsinized nucleosomal arrays form the 40S folding intermediate in ≥ 8 mM $MgCl_2$ suggests that the specific tail domains involved in mediating the 29S → 40S folding transition do so by a mechanism that involves DNA charge neutralization. Furthermore, the observation that both the fully trypsinized arrays and the hybrid arrays containing H2A/H2B tail domains exhibit the same extent of folding in 4 mM $MgCl_2$ while the arrays containing only the H3/H4 tail domains were significantly more folded under these conditions (Figure 6) suggests that the H3/H4 tail domains

are the dominant mediators of the 29S → 40S folding transition. This conclusion is consistent with the recent results of Moore and Ausio (1997). Finally, given that tail domain-mediated wrapping of nucleosomal core DNA can be replaced by ≤2 mM $MgCl_2$ (Fletcher & Hansen, 1995; Figure 4), and that the tail domains rearrange to a nonnucleosomal location during folding (Fletcher & Hansen, 1995), tail domain-mediated formation of the 40S structure must involve interactions with linker DNA and(or) the DNA of adjacent nucleosomal subunits.

Numerous lines of evidence indicate that the extensively folded 55S conformation of a 208-12 nucleosomal array is formed directly from the 40S folding intermediate [Schwarz & Hansen, 1994; Fletcher et al., 1994b; reviewed in Fletcher and Hansen (1996)]. Neither the fully trypsinized arrays nor the two hybrid trypsinized arrays could form the 55S conformation in any of the $MgCl_2$ conditions tested, despite the fact each of these arrays could form the 40S folding intermediate in ≥4 mM $MgCl_2$. This indicates that both the H2A/H2B and H3/H4 tail domains also must provide essential functions required for the 40S → 55S transition. However, the mechanism by which the tail domains mediate formation of the 55S conformation clearly is different than that involved in the 29S → 40S transition. In particular, formation of the 55S conformation is not dependent solely on tail domain-dependent DNA charge neutralization. Possible mechanisms that may be involved in formation of the 55S structure include tail domain interactions with the protein components of other nucleosomal subunits [e.g., other tail domains or exposed structured region(s) of the histone octamer], and(or) some type of protein−DNA interaction that cannot be replaced by high concentrations of divalent cations.

Mg^{2+}-dependent oligomerization, like intramolecular folding, also is strictly dependent on the tail domains. However, the fact that these two transitions are not strictly coupled (Schwarz et al., 1996) suggests that the mechanistic actions of the tail domains in oligomerization and folding are distinct. Each of the hybrid trypsinized arrays could completely oligomerize in the presence of Mg^{2+} whereas fully trypsinized nucleosomal arrays were essentially incapable of oligomerization at any $MgCl_2$ concentration (Figure 2). This is in direct contrast to the results of the folding studies, where neither hybrid array alone was capable of achieving maximal folding in high Mg^{2+} (see above). While intact nucleosomal arrays achieved complete oligomerization in ∼6 mM $MgCl_2$, hybrid trypsinized arrays containing only the H3/H4 or H2A/H2B tail domains required 10 mM and 25 mM $MgCl_2$, respectively. These data suggest that in an intact nucleosomal array, the H3/H4 tail domains are the primary mediators of oligomerization while the H2A/H2B dimers contribute to a much lesser extent. Interestingly, H3/H4 tetramer arrays lacking the entire H2A/H2B dimers have an oligomerization profile essentially identical to that of an intact array (Schwarz et al., 1996). One possible explanation for this result is that the exposed hydrophobic surfaces in a H3/H4 tetramer array (which are not present in the hybrid nucleosomal array containing trypsinized H2A/H2B dimers) facilitate oligomerization. Alternatively, the geometry of H3/H4 tail domains relative to the DNA path, which is substantively different in an H3/H4 tetramer array compared to an intact array (Hansen et al., 1991; Hansen & Wolffe, 1994), may be critical for oligomerization. In any case, the fact that no amount of $MgCl_2$ can induce oligomerization in the absence of the tail domains together with the observation that high [$MgCl_2$] is able to induce oligomerization when at least one set of tail domains is present suggests that the core histone N-termini mediate oligomerization through both electrostatic- and non-electrostatic-based mechanisms.

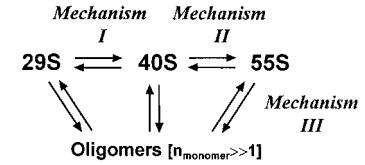

FIGURE 7: Complexity of involvement of the core histone tail domains in the solution-state conformational dynamics of intact 208-12 nucleosomal arrays. Three distinct mechanisms of action of the tail domains have been identified. See Discussion for details.

In summary, studies of the Mg^{2+}-dependent behavior of hybrid trypsinized nucleosomal arrays have revealed three distinct functions performed by the core histone N-terminal tails in nucleosomal array condensation. Each of these functions is essential for a specific aspect of compaction, and each appears to involve different molecular mechanisms of action (Figure 7). Mechanism I, which mediates the 29S → 40S folding transition, primarily involves DNA-charge neutralization by the H3/H4 tail domains. Mechanism II mediates the 40S → 55S folding transition. This mechanism requires contributions from both the H2A/H2B and H3/H4 tail domains and involves something other than simple tail-dependent charge neutralization. Mechanism III mediates cooperative oligomerization of nucleosomal arrays and in part involves non-electrostatic-based intermolecular interactions of tail domains with components of other nucleosomal array monomers. The exact nature of the non-electrostatic-based mechanisms involved in tail domain function during chromatin condensation remains to be elucidated. Nevertheless, when taken together, the simplest explanation for the observed complexity of tail domain function is that either each of the eight different N-termini of each nucleosomal subunit performs different mechanistic functions or the same tail domain mediates multiple functions through different molecular mechanisms. In this regard, it is important to note that recent genetic analyses of tail domain function in yeast [see Lenfant et al. (1996) and references cited therein] have revealed a level of complexity in the biological functions of each of the core histone N-termini in vivo that is consistent with the results reported here.

Competitive Interaction Model of Tail Domain Function in Chromatin. All of the key functions of the core histone N-termini involved in mediating chromatin condensation involve some type of intra- and(or) interarray interactions. In addition, it has recently been established that the H3 and H4 tail domains are capable of combinatorial interactions with the chromatin associated regulatory proteins SIR3 and SIR4 (Hecht et al., 1995, Hecht et al., 1996), and TUP1 (Edmondson et al., 1996). In the two latter cases, the nucleoprotein assembly formed from the linkage of the regulatory proteins with the chromatin fiber is associated with specific regulation of gene expression [reviewed in Roth (1995) and Kingston (1996)]. Thus, at this point any model of N-terminal domain function in chromatin must explain why the tail domains play essential roles in modulation of nucleosomal array structural dynamics, and at the same time bind to non-histone protein components of the chromosomal fiber. To reconcile these observations, we propose that the

observed functional complexity of tail domain action in chromatin can best be accounted for by a "competitive interaction" model in which the structural and functional properties of any given region of a chromosomal fiber are dictated largely by the nature of the tail domain interaction partners within that region. For example, in the absence of tail domain binding non-histone proteins, the N-termini will mediate the short- and long-range fiber interactions that lead to the structural and functional properties of classical 30 nm diameter chromatin (in this case linker histones are also present to stabilize the 30 nm fiber). However, when tail binding regulatory proteins are components of the fiber (e.g., SIR3, SIR4), those specific tail domains that are bound to the non-histone proteins will no longer be capable of mediating intrafiber interactions. This necessarily will lead to remodeling of the chromatin fiber and subsequent establishment of a specific chromosomal domain whose structure and function will be an amalgam of the properties of the regulatory protein(s) and the underlying nucleosomal array lacking certain key tail domain-mediated intrafiber functions [reviewed in Hansen (1997)]. Importantly, the complexity of tail domain function within the chromatin fiber, together with the ability of external regulatory proteins to alter these functions through competitive binding to the tail domains, allows the core histone N-termini to provide a direct molecular link that permits chromatin to be an *active* participant in regulation of the biological processes (e.g., transcription, replication, cell cycle control) that occur within the interphase chromosomal fiber.

ACKNOWLEDGMENT

We thank D. Goethke and C. Turgeon for technical support, and L. Carruthers for critically reading the manuscript.

REFERENCES

Ausio, J., Dong, F., & van Holde, K. E. (1989) *J. Mol. Biol. 206*, 451−463.
Belmont, A. S., & Bruce, K. (1994) *J. Cell Biol. 127*, 287−302.
Belmont, A. S., Braunfeld, M. B., Sedat, J. W., & Agard, D. A. (1989) *Chromosoma 98*, 129−143.
Bohm, L., & Crane-Robinson, C. (1984) *Biosci. Rep. 4*, 365−386.
Bouvet, P., Dimitrov, S., & Wolffe, A. P. (1994) *Genes Dev. 8*, 1147−1159.
Boy de la Tour, E., & Laemmli, U. K. (1988) *Cell 55*, 937−944.
Dasso, M., Dimitrov, S., & Wolffe, A. P. (1994) *Proc. Natl. Acad. Sci. U.S.A. 91*, 12477−12481.
Dong, F., Hansen, J. C., & van Holde, K. E. (1990) *Proc. Natl. Acad. Sci. U.S.A. 87*, 5724−5728.
Edmondson, D. G., Smith, M. M., & Roth, S. Y. (1996) *Genes Dev. 10*, 1247−1259.
Fletcher, T. M., & Hansen, J. C. (1995) *J. Biol. Chem. 270*, 25359−25362.
Fletcher, T. M., & Hansen, J. C. (1996) *Crit. Rev. Eukaryotic Gene Expression 6*, 149−188.
Fletcher, T. M., Krishnan, U., Serwer, P., & Hansen, J. C. (1994a) *Biochemistry 33*, 2226−2233.
Fletcher, T. M., Serwer, P., & Hansen, J. C. (1994b) *Biochemistry 33*, 10859−10863.
Garcia-Ramirez, M., Dong, F., & Ausio, J. (1992) *J. Biol. Chem. 267*, 19587−19595.
Hansen, J. C. (1997) *Chemtracts: Biochem. Mol. Biol. 10*, 56−69.
Hansen, J. C., & Wolffe, A. P. (1992) *Biochemistry 31*, 7977−7988.
Hansen, J. C., & Lohr, D. (1993) *J. Biol. Chem. 268*, 5840−5848.
Hansen, J. C., & Wolffe, A. P. (1994) *Proc. Natl. Acad. Sci. U.S.A. 91*, 2339−2343.
Hansen, J. C., Ausio, J., Stanik, V. H., & van Holde, K. E. (1989) *Biochemistry 28*, 9129−9136.
Hansen, J. C., van Holde, K. E., & Lohr, D. (1991) *J. Biol. Chem. 266*, 4276−4282.
Hansen, J. C., Lebowitz, J., & Demeler, B. (1994) *Biochemistry 33*, 13155−13163.
Hansen, J. C., Kreider, J. I., Demeler, B., & Fletcher, T. M. (1997) *Methods: Companion Methods Enzymol. 12*, 62−72.
Hecht, A., Laroche, T., Strahl-Bolsinger, S., Gasser, S. M., & Grunstein, M. (1995) *Cell 80*, 583−592.
Hecht, A., Strahl-Bolsinger, S., & Grunstein, M. (1996) *Nature 383*, 92−96.
Hirano, T., & Michison, T. J. (1994) *Cell 79*, 449−458.
Kingston, R. E., Bunker, C. A., & Imbalzano, A. N. (1996) *Genes Dev. 10*, 905−913.
Lenfant, F., Mann, R. K., Thomsen, B., Ling, X., & Grunstein, M. (1996) *EMBO J. 15*, 3974−3985.
Meersseman, G., Pennings, S., & Bradbury, E. M. (1991) *J. Mol. Biol. 220*, 89−100.
Meersseman, G., Pennings, S., & Bradbury, E. M. (1992) *EMBO J. 11*, 2951−2959.
Moore, S. C., & Ausio, J. (1997) *Biochem. Biophys. Res. Commun. 230*, 136−139.
Moudrianakis, E. N., & Arents, G. (1993) *Cold Spring Harbor Symp. Quant. Biol. 58*, 273−279.
Ohsumi, K., Katagiri, C., & Kishimoto, T. (1993) *Science 262*, 2033−2035.
Pennings, S., Meersseman, G., & Bradbury, E. M. (1991) *J. Mol. Biol. 220*, 101−110.
Roth, S. (1995) *Curr. Opin. Genet. Dev. 5*, 168−173.
Schwarz, P. M., & Hansen, J. C. (1994) *J. Biol. Chem. 269*, 16284−16289.
Schwarz, P. M., Felthauser, A., Fletcher, T. M., & Hansen, J. C. (1996) *Biochemistry 35*, 4009−4015.
Shen, X., Yu, L., Weir, J. W., & Gorovsky, M. A. (1995) *Cell 82*, 47−56.
Simon, R. T., & Felsenfeld, G. (1979) *Nucleic Acids Res. 6*, 689−696.
Simpson, R. T., Thoma, F., & Brubaker, J. M. (1985) *Cell 42*, 799−808.
Stein, A. (1979) *J. Mol. Biol. 130*, 103−134.
Usachenko, S. I., Bavykin, S. G., Gavin, I. M., & Bradbury, E. M. (1994) *Proc. Natl. Acad. Sci. U.S.A. 91*, 6845−6849.
van Holde, K. E. (1988) *Chromatin*, Springer-Verlag, New York.
van Holde, K. E., & Weicshet, W. O. (1978) *Biopolymers 17*, 1387−1403.
van Holde, K., & Zlatanova, J. (1995) *J. Biol. Chem. 270*, 8373−8376.
Wolffe, A. P. (1995) *Chromatin: Structure & Function*, 2nd ed., Academic Press, New York.
Woodcock, C. L., & Horowitz, R. A. (1995) *Trends Cell Biol. 5*, 272−277.

BI970801N